

UNCLASSIFIED

AD NUMBER
AD461332
NEW LIMITATION CHANGE
TO Approved for public release, distribution unlimited
FROM Distribution authorized to U.S. Gov't. agencies and their contractors; Administrative/Operational Use; APR 1965. Other requests shall be referred to Office of Naval Research, ATTN: Code 429, Arlington, VA 22203.
AUTHORITY
ONR ltr dtd 4 May 1977

THIS PAGE IS UNCLASSIFIED

UNCLASSIFIED

AD 4 6 1 3 3 2

DEFENSE DOCUMENTATION CENTER

FOR

SCIENTIFIC AND TECHNICAL INFORMATION

CAMERON STATION ALEXANDRIA, VIRGINIA

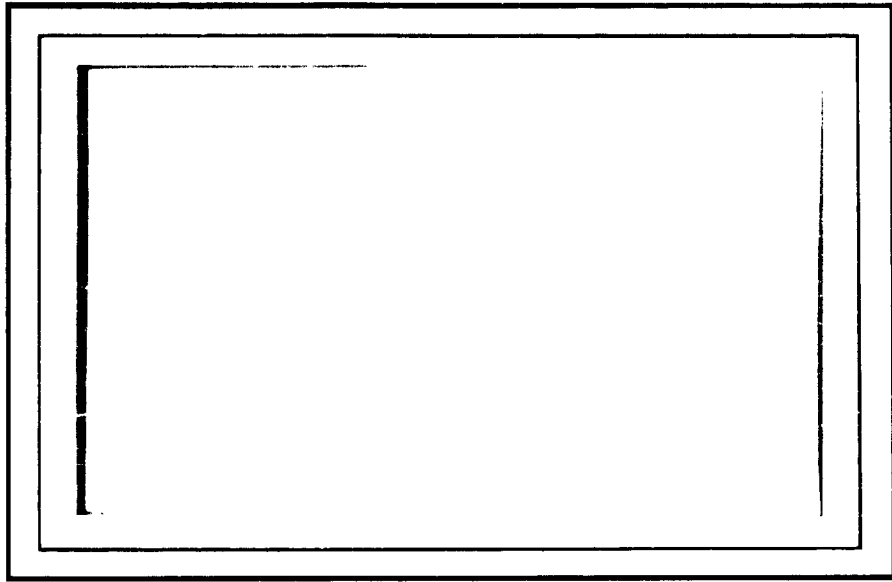


UNCLASSIFIED

NOTICE: When government or other drawings, specifications or other data are used for any purpose other than in connection with a definitely related government procurement operation, the U. S. Government thereby incurs no responsibility, nor any obligation whatsoever; and the fact that the Government may have formulated, furnished, or in any way supplied the said drawings, specifications, or other data is not to be regarded by implication or otherwise as in any manner licensing the holder or any other person or corporation, or conveying any rights or permission to manufacture, use or sell any patented invention that may in any way be related thereto.

4 6 1 3 3 2

CATALOGED BY: DDC  
AS AD No. 461332



DDC  
RECEIVED  
APR 22 1965  
DDC-IRA E



*AeroChem*

Research Laboratories, Inc.

a subsidiary of PFAUDLER PERMUTIT INC.

Princeton, New Jersey

ACOUSTIC ABSORPTION COEFFICIENTS  
OF THE COMBUSTION PRODUCTS OF  
ALUMINIZED PROPELLANTS

Final Report

A. Ribnick and H. F. Calcote

AeroChem Research Laboratories, Inc.

Princeton, New Jersey

a subsidiary of Pfaudler Permutit Inc.

Prepared for

OFFICE OF NAVAL RESEARCH

Contract Nonr 3477(00)

ARPA Order No. 23-62(25)

Project Code No. 9100

SUMMARY

A resonance tube method has been used to measure the absorption of sound passed through a column of propellant gases and solid particles produced by the burning of small samples of aluminized propellant. Aluminum composition was varied to observe the effect of the increased quantity of alumina particles on sound absorption. The acoustical absorption coefficient increased with increasing aluminum concentration in the propellant. The absorption coefficient increased linearly with the frequency, consistent with the particulate damping theory of Epstein and Carhart.<sup>2</sup> This theory was also used to estimate the sizes of alumina particles produced in the experiment. By a process of curve fitting, the inferred particle radii were either 0.80 or 3.5 microns, two solutions were possible. The initial average particle radius of the aluminum was 2.3 microns. Despite the fact that a statistical distribution of particle size was not considered in curve-fitting the data, the reasonableness of the calculated particle sizes lends further support to the Epstein and Carhart<sup>2</sup> theory.

TABLE OF CONTENTS

	<u>Page</u>
SUMMARY . . . . .	iii
LIST OF TABLES . . . . .	v
LIST OF FIGURES . . . . .	vi
NOMENCLATURE . . . . .	vii
INTRODUCTION . . . . .	1
THEORETICAL DISCUSSION . . . . .	2
EXPERIMENTAL TECHNIQUES . . . . .	4
Open-Tube Experiments . . . . .	5
Closed Resonance Tube Experiments . . . . .	5
EXPERIMENTAL RESULTS . . . . .	7
COMPARISON OF EXPERIMENT AND THEORY . . . . .	10
REFERENCES . . . . .	13

LIST OF TABLES

<u>Table</u>		<u>Page</u>
I	PROPELLANT COMPOSITIONS AND CALCULATED FLAME TEMPERATURE . . . . .	14
II	EFFECT OF ALUMINUM CONCENTRATION ON ABSORPTION COEFFICIENT . . . . .	15
III	PROPERTIES OF PROPELLANT GASES USED IN THE CALCULATION OF $\sigma$ . . . . .	16

LIST OF FIGURES

<u>Figure</u>		<u>Page</u>
1	VARIATION OF $f(z)$ WITH THE DIMENSIONLESS DISTANCE IN EPSTEIN-CARHART FORMULA . . . . .	17
2	ACOUSTIC RESONANCE TUBE AND PROPELLANT IGNITION SYSTEM . . . . .	18
3	FLOW CHART OF ACOUSTICAL AND ELECTRONIC EQUIPMENT.	19
4	EFFECT OF FREQUENCY ON ABSORPTION COEFFICIENT . . . . .	20
5	VARIATION IN ABSORPTION COEFFICIENT WITH TIME . . . . .	21
6	EFFECT OF ALUMINUM CONCENTRATION ON ACOUSTICAL ABSORPTION COEFFICIENT . . . . .	22
7	COMPARISON OF EXPERIMENTAL AND THEORETICAL ACOUSTIC ABSORPTION COEFFICIENTS . . . . .	23
8	COMPARISON OF EXPERIMENTAL AND THEORETICAL ACOUSTIC ABSORPTION COEFFICIENTS . . . . .	24
9	COMPARISON OF EXPERIMENTAL AND THEORETICAL ACOUSTIC ABSORPTION COEFFICIENTS . . . . .	25
10	COMPARISON OF EXPERIMENTAL AND THEORETICAL ACOUSTIC ABSORPTION COEFFICIENTS . . . . .	26

NOMENCLATURE

c	=	velocity of sound
f	=	frequency
$f_n$	=	frequency of n standing waves
$\Delta f$	=	resonant frequency range at half-power of peak resonant frequency
L	=	tube length
n	=	order of resonance or integer defining harmonics, cf. Eq. (4)
N	=	number density of particles
r	=	effective particle radius
T	=	absolute temperature
X	=	mole fraction
Z	=	$(\pi f / \nu)^{1/2} r$ , dimensionless particle size

Greek Symbols

$\delta$	=	ratio of gas density to particle density
$\eta$	=	viscosity of gas
$\nu$	=	kinematic viscosity of gas
$\bar{m}$	=	average molecular weight
$\sigma$	=	acoustical absorption coefficient, $\text{cm}^{-1}$

Subscript

i	=	individual components
---	---	-----------------------

## INTRODUCTION

Combustion instability in solid propellant rockets is a recurring problem which is being given much study. As has become clear, it is a complex resonance phenomenon intimately connected with the geometry of the system, the nature of the solid propellant, and a variety of other parameters. Frequently, it has been found that the onset of this condition can be controlled by the addition of certain additives to the fuel. The mechanism by which these additives work is by no means certain: they may be either chemically inert or may actually participate in the combustion process. For instance, one common additive--aluminum--forms aluminum oxide which, either as solid or liquid particles, acts to suppress the instability.<sup>1</sup> While the mechanism by which these particles act is not clearly established, it is apparent that the presence of particles in the acoustic field must lead to the absorption of field energy by the particles and thereby produce a damping effect on the undesirable resonances. If the damping effect is large enough, oscillations will not occur.

This report describes a series of experiments undertaken to measure the contribution of the alumina particles to the over-all damping in a solid propellant combustion exhaust. The experiments were designed to separate this effect from the other complicated interactions which occur in a real motor.

## THEORETICAL DISCUSSION

In a rocket motor combustion gas, acoustical energy may be absorbed by at least three mechanisms: absorption by walls, gases, and particles in the gas phase.

Acoustic absorption by the walls of a tube is proportional to the reciprocal of the tube diameter and to the square root of the frequency. It is also relatively small and, as the experimental values show, is unable to explain the rather large damping obtained here. Absorption by the gas itself is usually considered to be due to excitation of rotational degrees of freedom in the gas, therefore, it is not clear how it could be affected by addition of particles such as alumina. The measured values of absorptivity are too large to be explained by this phenomenon.

Epstein and Carhart<sup>2</sup> have developed a theory for the attenuation of sound by spherical particles suspended in a gas. In this theory, both the viscous and thermal dissipative losses are considered. Since the thermal losses for alumina particles are smaller than the viscous losses, only viscous losses will be considered here. With this simplification the following relationship for the acoustic absorption coefficient is obtained<sup>2</sup>:

$$\sigma = (6\pi\nu/c) Nr F(Z, \delta) \quad (1)$$

where:

$$F(Z, \delta) \equiv (1 + Z) \frac{16Z^4}{16Z^4 + 72\delta Z^3 + 81\delta^2(1 + 2Z + 2Z^2)} \quad (2)$$

$$Z \equiv (\pi f / \nu)^{1/2} r \quad (3)$$

The theoretical expression may now be examined to understand how the absorption coefficient may vary with particle number density,  $N$ , sound frequency,  $f$ , and particle radius,  $r$ . The coefficient  $\sigma$  will vary linearly with the particle number density, provided (in actual combustion systems) the particle radii do not differ appreciably as the aluminum concentration is varied. In order for  $N$  to vary linearly with the aluminum concentration, it is assumed that the aluminum is burned completely to its oxide. Sehgal<sup>3</sup> has reported that the average particle sizes of aluminum particles are not changed appreciably by a change in aluminum content from 12 to 18 wt.%. One might expect, therefore, that  $\sigma$  will vary linearly with the aluminum concentration.

By assuming a constant alumina particle radius and kinematic viscosity of the propellant gases, it may be shown that in the  $Z$  range of interest ( $Z < 1$ )  $\sigma \propto f^n$ , where the exponent  $n$  varies from two ( $Z \ll 1$ ) to, effectively, zero ( $Z$  "large"). Therefore, for certain fixed particle sizes, it may be possible to observe an absorption coefficient which varies as the frequency squared to one which is independent of sound frequency. In particular, a (locally) linear variation of  $\sigma$  with  $f$  may also be expected. This behavior is illustrated in Fig. 1 where calculated values of  $F(Z)$  for the particular propellants under consideration are plotted against  $Z$  on logarithmic coordinates. It will be observed that the lowest

values of  $Z$  give a line with a slope approaching 4 asymptotically, while for higher values of  $Z$ ,  $F(Z)$  approaches zero slope.\* Between these two extremes, the curve shows a rather sharp break near  $Z \approx 0.01$ , where the slope changes monotonically and rapidly from almost 4 to almost 0. This indicates that, for fixed values of  $r$  and  $\nu$ ,  $\sigma$  varies as  $f^2$  for low values of  $Z$  but becomes essentially independent of frequency at somewhat larger values.

The Epstein-Carhart formula also states that for a fixed mass fraction of particles the absorption coefficient  $\sigma$  varies with the square of the particle size in the small  $Z$  extreme. However, for larger values of  $Z$ , the coefficient  $\sigma$  will vary inversely as the square of the particle size. Hence a maximum absorption coefficient is theoretically predictable for an optimum particle size. For alumina particles suspended in the propellant product gases at a pressure of 200 psi, Horton and McGie<sup>1</sup> have estimated the optimum particle radius to be 1.5 microns.

The parameters  $N$  and  $\delta$  are sensitive to a variation in temperature because of their relation to gas density. When all variables sensitive to temperature change are considered (including the sound speed  $c$ ) the absorption coefficient is found to vary as about  $T^{-1}$ .

At fixed particle mass fraction and particle size pressure does not affect  $\sigma$  because the gas particle density and kinematic viscosity pressure-dependence cancel, but in practice pressure may nevertheless influence the particulate damping process. Sehgal<sup>3</sup> has shown that the pressure level in an experimental strand test motor exerted an influence on the average particle radii of alumina produced in these burning tests. He reported that the average alumina particle size increased linearly with the pressure in a range of pressures from 15 to 1000 psi. Since sound absorption is strongly dependent on particle size, pressure can thus exert a strong influence on the particulate damping process through its control of the sizes of particles produced in the burning process. One is led to conclude that the mean pressure in the rocket motor has no effect on the gaseous acoustical damping but

---

\* If one considered still larger values of  $Z$  then  $F$  would ultimately increase linearly with  $Z$ , however, these values of  $Z$  are not of interest here.

apparently regulates the particulate damping process via the above mechanism. Along with this interpretation of Sehgal's work goes the fact, supported by the Epstein-Carhart theory, that there is an optimum particle size which can produce a maximum absorption coefficient. Consideration of this would mean there is also an optimum pressure which is associated with a maximum of sound absorption.

In this discussion of particulate damping, it has been shown how  $\sigma$  might be affected by aluminum concentration, frequency, temperature, pressure, and particle radius. The theory predicts a linear dependence on aluminum concentration, a varying dependence on temperature and radius, and a small dependence on pressure when pressure does not influence particle size. For very small particle sizes, acoustic damping can become small compared with the other damping processes. However, within the range of particle sizes and frequencies experienced in this study ( $0.5 \leq r \leq 4 \mu$ ;  $0.6 \leq f \leq 4 \text{ Kc/sec}$ ) particulate damping can be the dominating dissipative mechanism.

In any practical case, a range of particle sizes will exist, so that this theory-- which is for single-sized particles--will require modification.

#### EXPERIMENTAL TECHNIQUES

It is usually assumed that acoustic instabilities are driven by complicated non-linear couplings between the sound field and the flame front in the rocket motor. As a result, it is most difficult to separate flame front effects from those produced by the propellant exhaust gases in measurements made in typical motors. In order to avoid this problem, the experiments were so designed that the flame front did not contribute to the acoustic field. Instead, the sound waves were generated by an acoustic driver, while the solid propellant charge served only to supply the exhaust gases whose acoustic absorption it was desired to measure.

### Open-Tube Experiments

A simple open-tube technique was used in a first attempt to determine the relative sound absorption of the combustion products of aluminized and nonaluminized propellants. The apparatus consisted of a brass pipe 91.5 cm long with a probe microphone attached midway along its length. A 60-watt acoustic driver was coupled to one end of the pipe, while a replaceable propellant cartridge was located near the other end of the pipe through which sound waves passed. The variation in sound intensity with time as measured by the microphone was recorded on a strip chart as combustion gases from a burning solid propellant filled the tube. These tests were run at a number of frequencies, not necessarily resonant with the tube. In this way, relative sound intensity for a 5 wt. % aluminum concentration were determined to be 15 db below those of a nonaluminized propellant. With higher concentrations of aluminum, the loss rose even higher but appeared to level off at 10 wt. % aluminum, although concentrations as high as 20 wt. % were tested.

Accurate interpretation of data from these experiments was difficult, however. Considerable uncertainty was introduced because different degrees of coupling between driver and gas and between gas and microphone might well have occurred as the gas composition changed. The physical state of the combustion gases was not well defined, and minor resonances and background noise contributed to the over-all uncertainty. For this reason, a closed resonance tube technique was used.

### Closed Resonance Tube Experiments

The bulk of the data were obtained using a closed-tube apparatus adapted from an acoustic experiment of Parker.<sup>4</sup> This technique depends upon measuring the resonant frequency for standing waves in a tube of variable length. The relative width of a resonance frequency curve is measured, which is equivalent to measuring the "Q" of the system. Since the relative width of the frequency curve depends primarily on the dissipation of energy in the tube and only weakly on other parameters, interpretation of the data is greatly simplified.

A rigid-wall copper tube was used (Fig. 2) 90 cm in length and 3.8 cm in diameter. A 1-gm cube of solid propellant was positioned near the center of the tube and ignited electrically. At one end of the tube, a short section of narrower tube filled with straight steel wires served as a coupling tube to an acoustic driver. This coupling technique afforded a uniform distribution of sound in the resonance chamber and also provided a high source impedance.\* The length of the tube could be varied to obtain a series of resonant lengths by a movable piston which adjusted the resonance frequency of the assembly. A dynamic crystal microphone was mounted on this piston and mechanically isolated from the piston by a cork sleeve.

Resonance in a closed tube is established when a series of standing waves of frequency,  $f_n$ , are contained within the tube. This condition occurs when the frequency is:

$$f_n = nc/2L \quad (n = 1, 2, \dots) \quad (4)$$

When the propellant starts to burn, a new gaseous medium displaces the original air and a new series of standing waves appear in the tube. In actual experiments, the resonant frequency shifts to somewhat higher values because of the lower density or the higher speed of sound in the propellant gases.

Sound absorption was measured as follows: A desirable resonant frequency was first established in air and the driver frequency was swept automatically at a rate of 16 cps approximately 50 cps on either side of the resonant frequency. The sweep was from low to high frequency and then reversed to remove any hysteresis problems. The microphone response was recorded with time and displayed a peak output each time the frequency passed through resonance. Determination of the acoustical absorption coefficient involved measurement of peak width at the "half-power" points of the resonant curve together with the determination of the resonant frequency. The acoustical absorption coefficient is then given by the expression:

---

\* Other forms of coupling, including direct coupling, were also tried with little real difference in results.

$$\sigma = \pi \Delta f / c$$

or since  $c = 2f_n L/n$

$$\sigma = (\pi n / 2L) (\Delta f / f_n) \quad (5)$$

where  $\Delta f$  is the resonant frequency range at the half-power points. The order of resonance,  $n$ , was determined from the resonance peak measurements in air, since  $f_n$ ,  $c$ , and  $L$  are then known in Eq. (4). Knowing  $n$ , the value of  $c$  for any particular gas or gas mixtures was determined.

A block diagram of the instrumentation is given in Fig. 3. Driver input was obtained through a power amplifier from the signal generator of a Hewlett-Packard Model 500 (1% of full scale, 100Kc) wave analyzer whose frequency was recorded on one channel of a dual-channel Sanborn Model 322 recorder. Output of the microphone passed through a wave analyzer (acting as a filter) and was recorded on the other channel of the recorder. The recordings therefore gave simultaneous measurements of frequency and microphone response at all times.

Upon ignition of the solid propellant, the resonant frequency of the tube could be observed to change, as well as the relative peak shape and peak heights. A series of such peaks were recorded for each run to determine the time response of the system. Propellant samples tested were composite mixtures of ammonium perchlorate oxidizer and polystyrene fuel. In order to incorporate varying amounts of aluminum, the basic composition (78 wt. %  $\text{NH}_4\text{ClO}_4$ -22 wt. % polystyrene) was changed in the manner shown in Table I. This composition change produced a  $310^\circ\text{K}$  change in the calculated adiabatic flame temperatures at the two extremes (0 and 10% aluminum).

### EXPERIMENTAL RESULTS

Acoustical absorption coefficients were evaluated by a series of runs in the closed-tube experiments. The first experiments were done with the nonaluminized propellant and are presented in Fig. 4 with results from Horton and McGie<sup>1</sup> and theoretical curves. The Horton and McGie data were obtained at 14 atm total pressure, and our data were obtained at 1 atm. The propellant employed by Horton and McGie was: 80 wt. % ammonium perchlorate, 18 wt. % polybutadiene polyacrylic

acid, and 2 wt. % copper chromite. The theoretical curves were computed with the Helmholtz-Kirchoff equation for a plane wave in a tube with damping using the calculated adiabatic flame temperatures and corresponding gas compositions.

The two experimental results are rather similar. The deviation from theory is not understood but is probably due in part to a lower-than-calculated temperature.

In order to further understand the interrelationship of the various parameters involved in these measurements, a group of studies was conducted to determine the change in absorption with time in the resonance tube. Studies for 5 wt. % aluminum samples in both an open and a closed tube and 0 wt. % aluminum in an open tube, are presented in Fig. 5; in the closed tube, pressures rose to 2.04 atm following propellant ignition, whereas in the open tube the pressure remained at atmospheric. It was observed that an initial sharp drop in absorption occurred in the open tube well within the first 100 sec followed by a much slower decrease over an extended period. The sharp drop was not nearly so evident in the closed tube, with the final portions of the two curves having essentially identical slopes. No explanation for the difference in the initial portion of the curves is proposed. Experimental details make measurement of  $\Delta f$  difficult at any time earlier than 10 sec after burning ceases, so that the initial portion of the curve is somewhat dubious. The central resonant frequency, 3100 cps, did not change appreciably over the indicated time period so that the time variation of  $\Delta f$  corresponds to a time variation of the absorption coefficient  $\sigma$ . In this time, the  $\Delta f$  value would have shifted about 7 cps. This could represent an error of about 10% in the measurements reported here and would always represent a lower absorption coefficient than the true value. It does appear that in the open-tube experiments the absorption coefficient decreased in an exponential manner for the first 60 sec with a half-life of about 45 sec. For the next 15 min the absorption decreased exponentially with a half-life of about 700 sec. The only effect of burning at a slightly higher pressure was to make the initial period of drop of doubtful significance, without much effect on the long-time rate of change. It is not clear whether the initial drop occurred more rapidly or not at all.

The change with time may be due to several possible effects: (1) a decrease in the total number of particles interacting due to settling or agglomeration, (2) a change in average particle radius due to a differential settling rate among the various sizes of particles present, (3) a change in average radius of particles due to agglomeration of particles, and (4) a change in absorption due to changes in ambient conditions of the exhaust gas, i. e., changes in temperature, pressure, composition, etc. (Note in Fig. 5 that the rate of decay is the same with and without aluminum.)

While it will be shown that  $\sigma$  will be most sensitive to changes in particle radius, very large changes in temperature will still occur as the particles cool off, so that temperature could also be significant. It is evident that the change in time of the absorption coefficient will be a major complication in this experiment. Should future work be done with this technique, this complication will have to be given more attention than was possible here.

The results with various concentrations of aluminum are given in Table II. The absorption coefficients are plotted against aluminum concentration in Fig. 6. The values of  $\Delta f$  and  $f$  represent an average of several experimental runs. The mean deviations given with  $\Delta f$ ,  $f$  and  $\sigma$  increases significantly with increasing aluminum content, particularly at higher resonant frequencies.

The absorption of sound is expected to increase linearly with aluminum concentration if the particle size remains constant, i. e., the number density of particles varies linearly with aluminum concentration. It has been observed by H. Silla of this Laboratory that aluminized propellants burn inefficiently in 1 atm of nitrogen. Rough estimates indicate that only 60 wt. % of the aluminum is burned. At high (about 10%) concentrations of aluminum, the efficiency is less than at lower concentrations. Thus, the lack of linearity in Fig. 5 may be due to inefficient combustion of aluminum which would be expected to produce a different particle size.

COMPARISON OF EXPERIMENT AND THEORY

Equation (1) was used to calculate a theoretical  $\sigma$  in order to compare with measured values from the resonance tube technique.

The various properties of the propellant gases (density, viscosity, particle number density, etc.) were derived from thermodynamic calculations of the adiabatic flame temperature. The viscosity of the gaseous mixtures was calculated from the approximate formula

$$\eta = (1/\mu) \sum_i X_i \mu_i \eta_i \quad (6)$$

The individual gas viscosities,  $\eta_i$ , were taken from the viscosity-temperature tables assembled by Svehla.<sup>5</sup> The alumina particle density was assumed to be 4.0 gm/cm<sup>3</sup>, the same as the bulk density of Al<sub>2</sub>O<sub>3</sub>.

Table III lists the calculated gas properties. Expressions for N and  $\sigma$  are also given. The expression for  $\sigma$  is simplified in terms of the function F(Z) and r, both unknown quantities. The expression for  $\sigma$  is:

$$\sigma = \text{constant} \cdot F(Z)/r^2 \quad (7)$$

The constant in Eq. (7) is the term  $(6\pi\nu/c)N$  appearing in Eq. (1), which has now been calculated.

The function of F(Z) may be estimated by assigning arbitrarily chosen values of Z and the calculated ratio of gas to particle density,  $\delta$ . Figure 1 describes the variation of the function F(Z) in terms of Z. Note the curve has a steep slope where Z has values of  $5 \times 10^{-3}$  and lower. As Z increases, the slope of the curve progressively decreases to values near zero. Since Z depends linearly on r and  $f^{1/2}$ ,  $\sigma$  may be expected to vary with frequency when r is constant, according to the value of the slope of the F(Z) vs. Z curve. If the slope is 4,  $\sigma$  will vary as the frequency squared. A slope of 2 will produce a linear variation with frequency. A slope of zero means that  $\sigma$  is independent of the frequency.

The observed absorption coefficients are plotted as  $\sigma$  vs.  $f$  in Figs. 7 to 10. The observed slopes of unity displayed by the experimental curves show that the composition of the gases and particles is such as to produce a  $Z$  with a value nearly  $10^{-2}$ , where  $\sigma$  varies as  $Z^2$  or  $f$  (Fig. 1).

It was possible to calculate  $\sigma$  using Eq. (1) and Fig. 1. In this calculation, various values of particle radii were assumed and the experimental frequencies were used. One experimental  $\sigma$  was then fitted (at a frequency of 3070 cps) with a calculated  $\sigma$ . Once this experimental point was fitted,  $r$  was fixed and other  $\sigma$ 's were calculated corresponding to other frequencies, and these absorption coefficients were compared with those actually measured by the resonance tube technique.

Figures 7 and 8 show this comparison of observed and calculated  $\sigma$  as a function of frequency; both variables are plotted on logarithmic coordinates. It is apparent that the experimental points form a straight line of slope unity, which passes generally between the two curves calculated from the theoretical expression for  $\sigma$ . Since the two calculated curves represent assumed small and large particle sizes (both of which fit the experimental  $\sigma$  at 3070 cycles/sec), it is impossible to decide on which particle size corresponds to reality.

Figures 7 and 8 display the calculated values of  $\sigma$  for propellant gases assumed to be near the adiabatic flame temperatures,  $2730^{\circ}\text{K}$  and  $2870^{\circ}\text{K}$ , for the 5 and 10 wt. % aluminum concentrations, respectively. This temperature may be too high, since appreciable cooling of the propellant gases must have taken place in the resonance tube.

To observe the effect of a lower temperature, the above calculation was repeated for a temperature of  $1000^{\circ}\text{K}$ , where corrections were applied to viscosity, gas density, velocity of sound, and all other parameters which might be affected by a decrease in temperature. Figures 9 and 10 show the results of this calculation. There is somewhat closer agreement of the calculated and experimental curves for the two propellants, but, again, the experimental curve is approximately an average of the curves calculated from theory.

It is again impossible to determine which particle size represents reality. A calculation was also carried out at 500°K with no improvement in the agreement of  $\sigma$  (observed) and  $\sigma$  (calculated).

For the 5 wt. % aluminum concentration, the small particle radius was calculated to be 0.95 micron and the large particle radius was calculated to be 3.4 microns. The 10 wt. % aluminum concentration produces a greater difference in particle radii, 0.55 and 3.8 microns.

Particle number densities vary from  $10^4$  to  $10^7$  particles/cm<sup>3</sup> for the large and small particles, respectively. Horton and McGie<sup>3</sup> have calculated a particle number density of  $10^7$  cm<sup>-3</sup> for a propellant containing 1% Al, where  $r$  was 0.6 microns. A comparison with their calculation of particle number density is offered only to show that the calculations given here are reasonable. As noted earlier larger particle number densities obtained for smaller particle radii cannot be interpreted to mean that a larger absorption of sound is theoretically possible for smaller particles. Size must also be considered in the light of the previously discussed existence of an optimum particle size producing a maximum of sound absorption. This optimum radius, as calculated by Horton and McGie,<sup>1</sup> is 1.5 microns for alumina particles, for propellant compositions of unusually low concentrations of aluminum (0 to 1.5 wt. %) and for combustion carried out at a pressure of 200 psi. In our investigation, in which propellants contained as much as 10 wt. % aluminum and were burned at 1 atm pressure, one might reasonably expect a larger particle size to be produced and also that the optimum particle radius would be somewhat larger than 1.5 microns.

The two possible average particle radii inferred from these experiments are 0.80 and 3.5 microns averaged from the results reported in Figs. 7 through 10:

<u>Small radii</u>	<u>Large radii</u>
1.7 microns	3.0 microns
1.0	4.0
0.95	3.4
0.55	3.8

The initial average particle radius of the aluminum used was 2.3 microns. These fall well within the domain of particle sizes which have been observed directly<sup>3</sup> and this in itself gives confidence to the experiment and procedure.

The experimental work should be repeated more carefully and analyzed using a theory valid for a statistical size distribution of particles. These were only preliminary experiments which demonstrate the possible utility of the method.

REFERENCES

1. Horton, M. D. and McGie, M. R., "Particulate Damping of Oscillating Combustion," AIAA J. 1, 1326 (1963).
2. Epstein, P. S. and Carhart, R. R., "The Absorption of Sound in Suspensions and Emulsions I. Water Fog in Air," J. Acoust. Soc. Am. 25, 533 (1953).
3. Sehgal, R., "An Experimental Investigation of a Gas-Particle System," JPL Technical Report No. 32-238, March 1962.
4. Parker, J. G., "Effect of Several Light Molecules on the Vibrational Relaxation Time of Oxygen," J. Chem. Phys. 34, 1767 (1961).
5. Svehla, R., "Estimated Viscosities and Thermal Conductivities of Gases at High Temperatures," (Lewis Research Center) NASA Tech. Report No. R-132 (1962).

TABLE I

PROPELLANT COMPOSITIONS AND CALCULATED FLAME TEMPERATURE

<u>Al, wt. %</u>	<u>NH<sub>4</sub>ClO<sub>4</sub>, wt. %</u>	<u>P-13, * wt. %</u>	<u>T, °K</u>	<u>Gas viscosity poise</u>	<u>Gas density, 10<sup>-4</sup> x gm/cm<sup>3</sup></u>
0.0	78.0	22.0	2560	8.09	1.12
2.0	76.4	21.6	----	----	----
4.0	74.9	21.1	----	----	----
5.0	74.1	20.9	2730	8.63	1.09
8.0	71.7	20.3	----	----	----
10.0	70.2	19.8	2870	6.36	1.07

---

\* Polystyrene

TABLE II

EFFECT OF ALUMINUM CONCENTRATION ON ABSORPTION COEFFICIENT

<u>Aluminum,</u> <u>wt. %</u>	<u>Frequency,</u> <u>cps*</u>	<u>Frequency width,</u> <u>cps*</u>	<u>Velocity of sound,</u> <u>10<sup>4</sup> cm/sec*</u>	<u><math>\sigma</math>, abs coeff,</u> <u>10<sup>-3</sup> cm<sup>-1</sup>*</u>
0.0	645 ± 7	26.0 ± 3.0	3.59 ± 0.04	2.26 ± 0.32
2.0	643 ± 10	26.0 ± 3.0	3.60 ± 0.05	2.24 ± 0.32
4.0	650 ± 4	29.0 ± 7.0	3.64 ± 0.02	2.48 ± 0.61
5.0	649 ± 2	30.0 ± 8.0	3.63 ± 0.01	2.58 ± 0.65
8.0	644 ± 0	29.0 ± 3.0	3.60 ± 0.00	2.56 ± 0.25
10.0	658 ± 4	33.0 ± 5.0	3.68 ± 0.02	2.85 ± 0.40
0.0	1570 ± 10	23.0 ± 2.0	3.53 ± 0.01	2.00 ± 0.74
5.0	1560 ± 20	63.0 ± 0.5	3.48 ± 0.02	5.53 ± 0.82
10.0	1560 ± 0	65.1 ± 0.0	3.50 ± 0.0	5.70 ± 0.29
0.0	3077 ± 21	44.0 ± 5.0	3.44 ± 0.02	4.17 ± 0.41
2.0	3090 ± 7	50.0 ± 3.0	3.45 ± 0.01	4.51 ± 0.28
5.0	3050 ± 0	83.0 ± 2.0	3.42 ± 0.00	7.61 ± 0.16
8.0	3070 ± 0	105 ± 7.0	3.44 ± 0.00	9.64 ± 0.60
10.0	3060 ± 10	107 ± 7.0	3.43 ± 0.01	9.70 ± 0.68
0.0	4020 ± 10	79.3 ± 1.1	3.68 ± 0.02	6.68 ± 0.20
5.0	4035 ± 35	15.5 ± 2.0	3.72 ± 0.02	12.9 ± 0.30

\*  
( ± mean deviation)

TABLE III  
PROPERTIES OF PROPELLANT GASES USED IN THE  
CALCULATION OF  $\sigma$

Composition of Propellant	74.1 (AP)-20.9 styrene fuel 5 Al	70.2 (AP)-9.8 styrene fuel 10 Al
Flame Temperature, T	2730°K	2870°K
Gas Density, gm/cm <sup>3</sup> , $\rho$	1.09	1.07
Viscosity, (poise) $\eta$	8.63	6.36
Kinematic Viscosity, cm <sup>2</sup> /sec, $\nu$	7.9	5.94
Speed of Sound, cm/sec, c	$1.07 \times 10^5$	$1.08 \times 10^5$
Ratio of gas to Particle Density,	$2.73 \times 10^{-5}$	$2.68 \times 10^{-5}$
Mass of Aluminum Oxide, gm, ms	0.095	0.190
Mass of Gases, gm, mg	0.905	0.810
Particle Number Density cm <sup>-3</sup> , N	$\frac{6.83 \times 10^{-7}}{r^3}$	$\frac{1.49 \times 10^{-6}}{r^3}$
Acoustic Absorption Coefficient, calc.	$\frac{9.45 \times 10^{-10} F(Z)}{r^2}$	$\frac{1.58 \times 10^{-9} F(Z)}{r^2}$

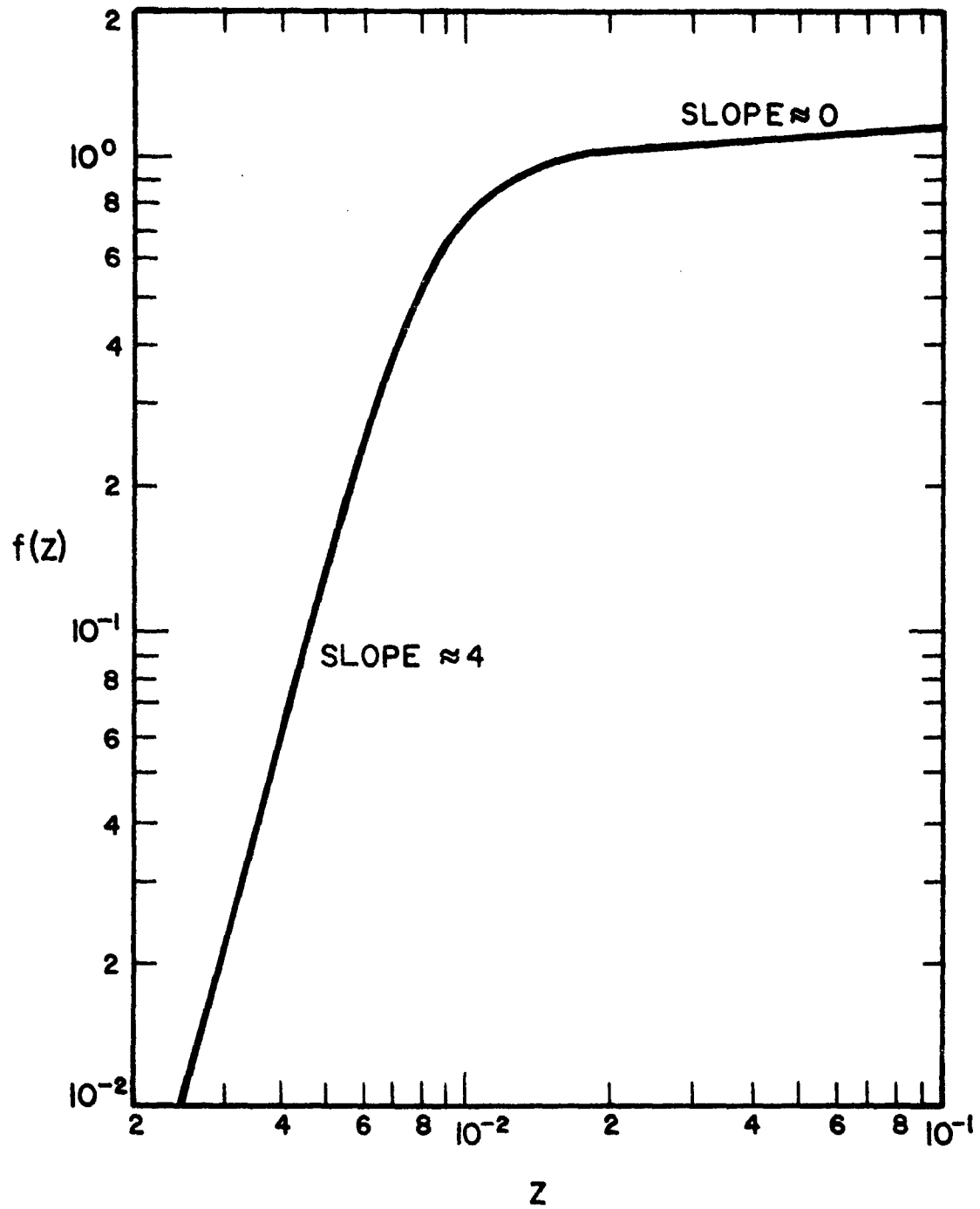


FIG. 1 VARIATION OF  $f(Z)$  WITH THE DIMENSIONLESS DISTANCE  
IN EPSTEIN-CARHART FORMULA

Assumed t wt. % Al,  $T = 2700^{\circ}\text{K}$ ,  $P = 1 \text{ atm}$ ,  
corresponding to  $\delta = 2.73 \times 10^{-5}$

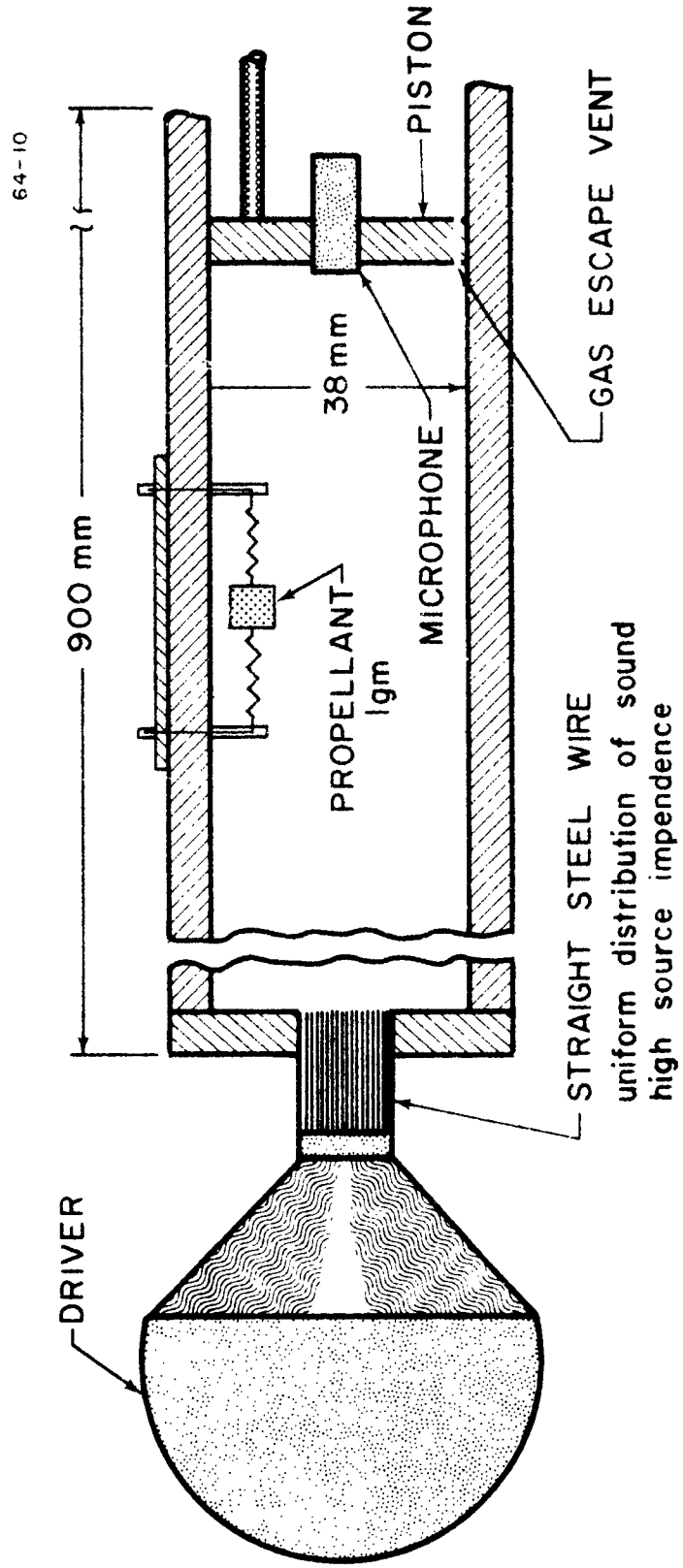


FIG. 7. ACOUSTIC RESONANCE TUBE AND PROPELLANT IGNITION SYSTEM

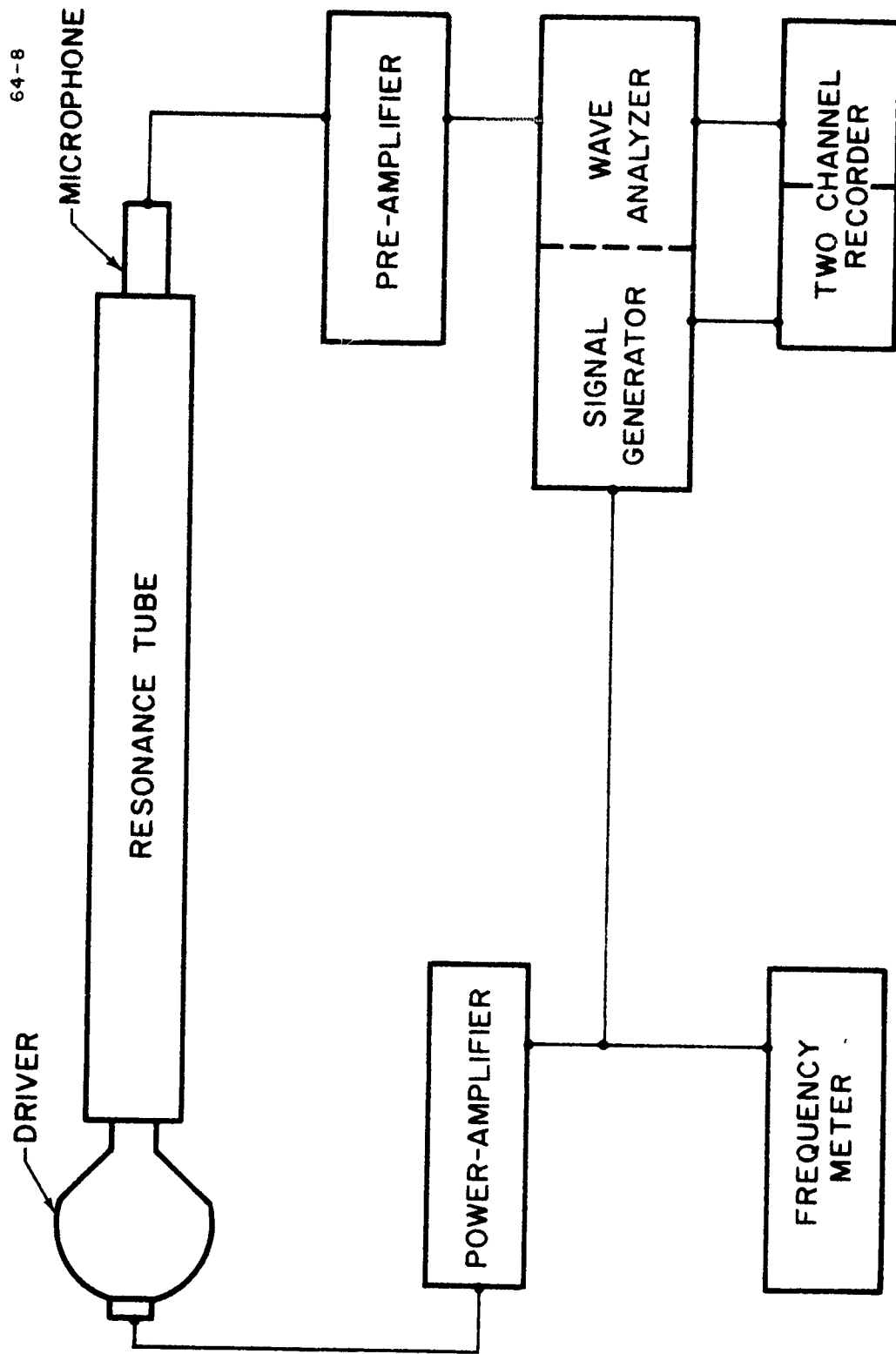


FIG. 3 FLOW CHART OF ACOUSTICAL AND ELECTRONIC EQUIPMENT

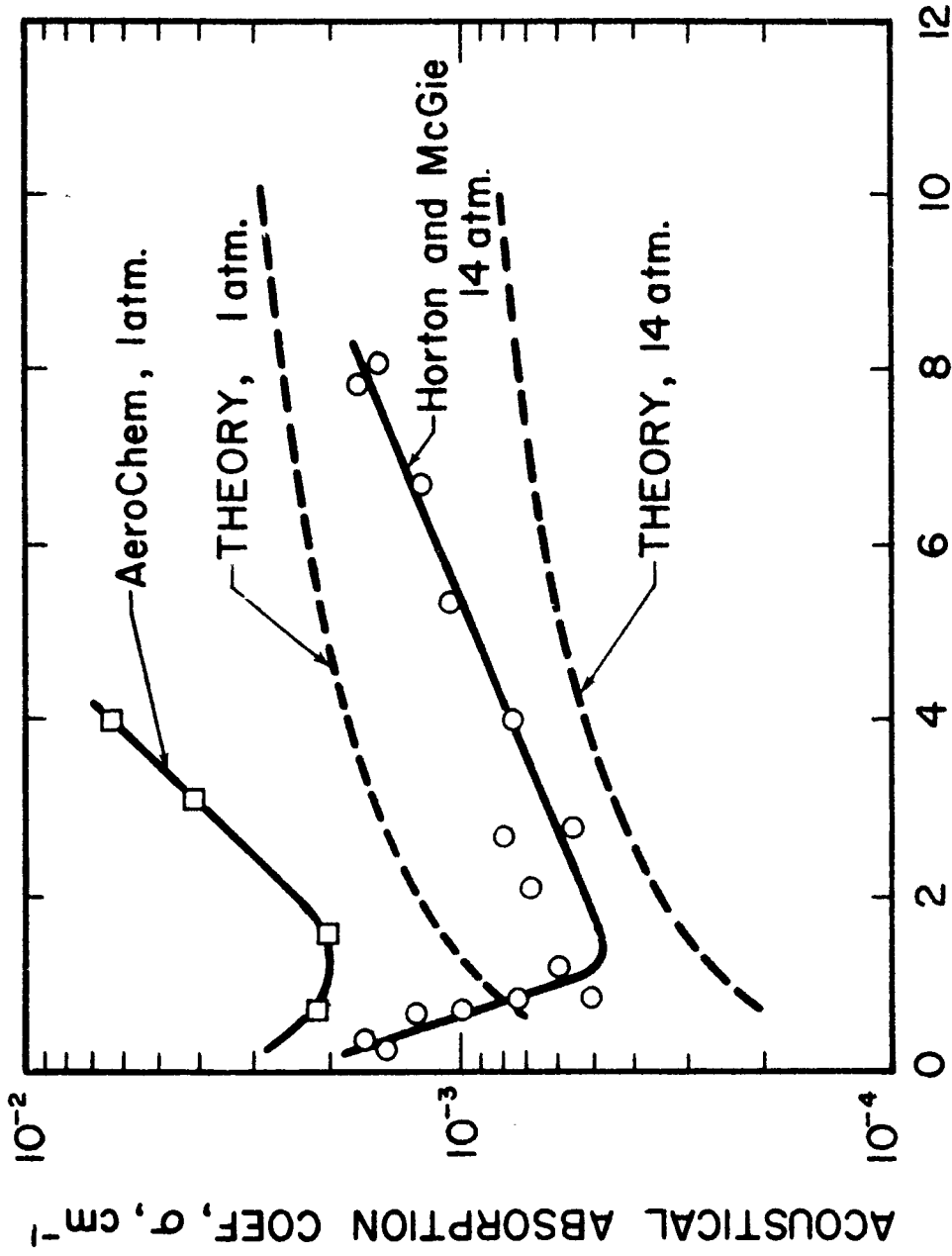


FIG. 4 EFFECT OF FREQUENCY ON ABSORPTION COEFFICIENT  
Aluminized propellant

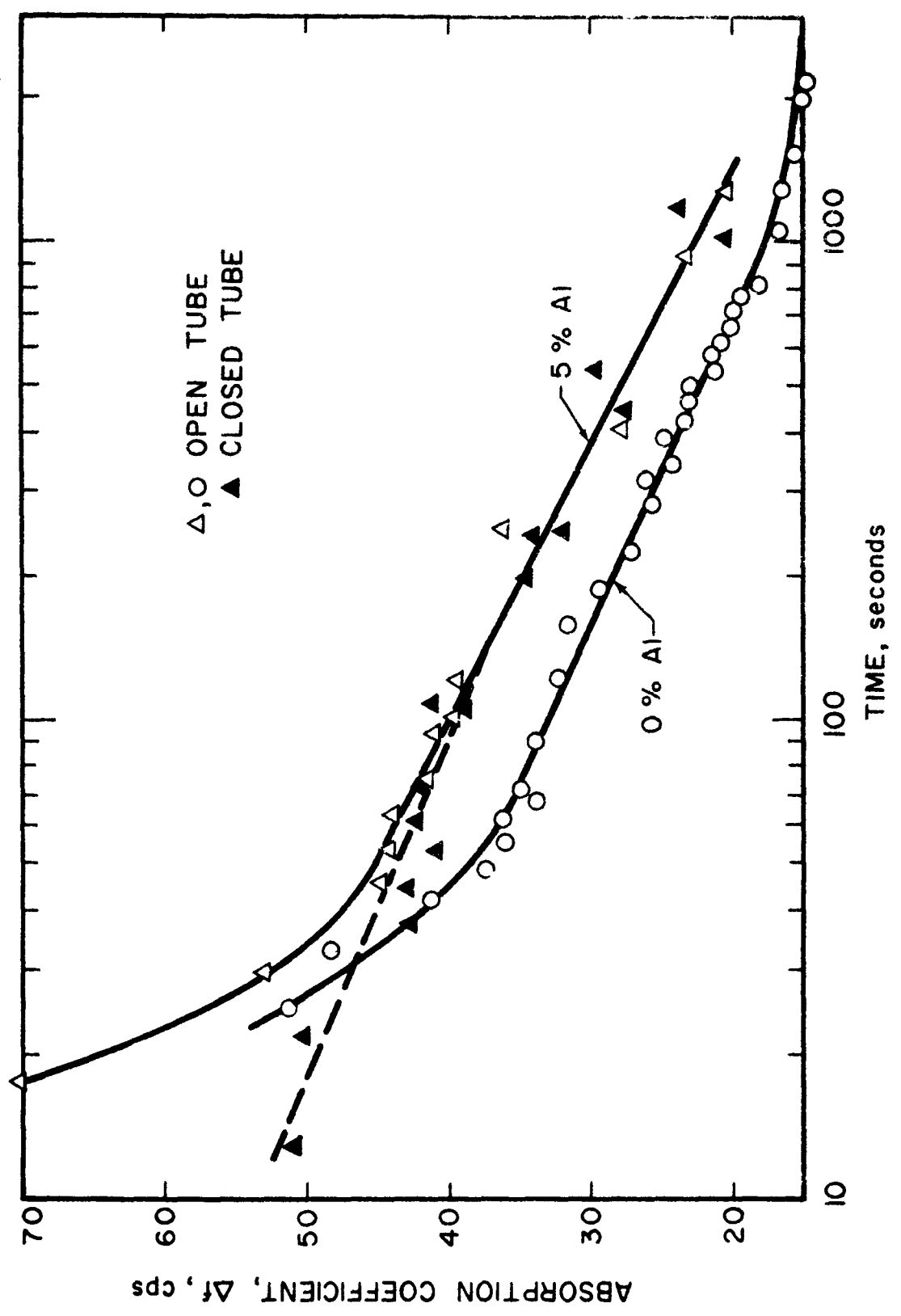


FIG. 5 VARIATION IN ABSORPTION COEFFICIENT WITH TIME AFTER IGNITION

Frequency = 3100 cps

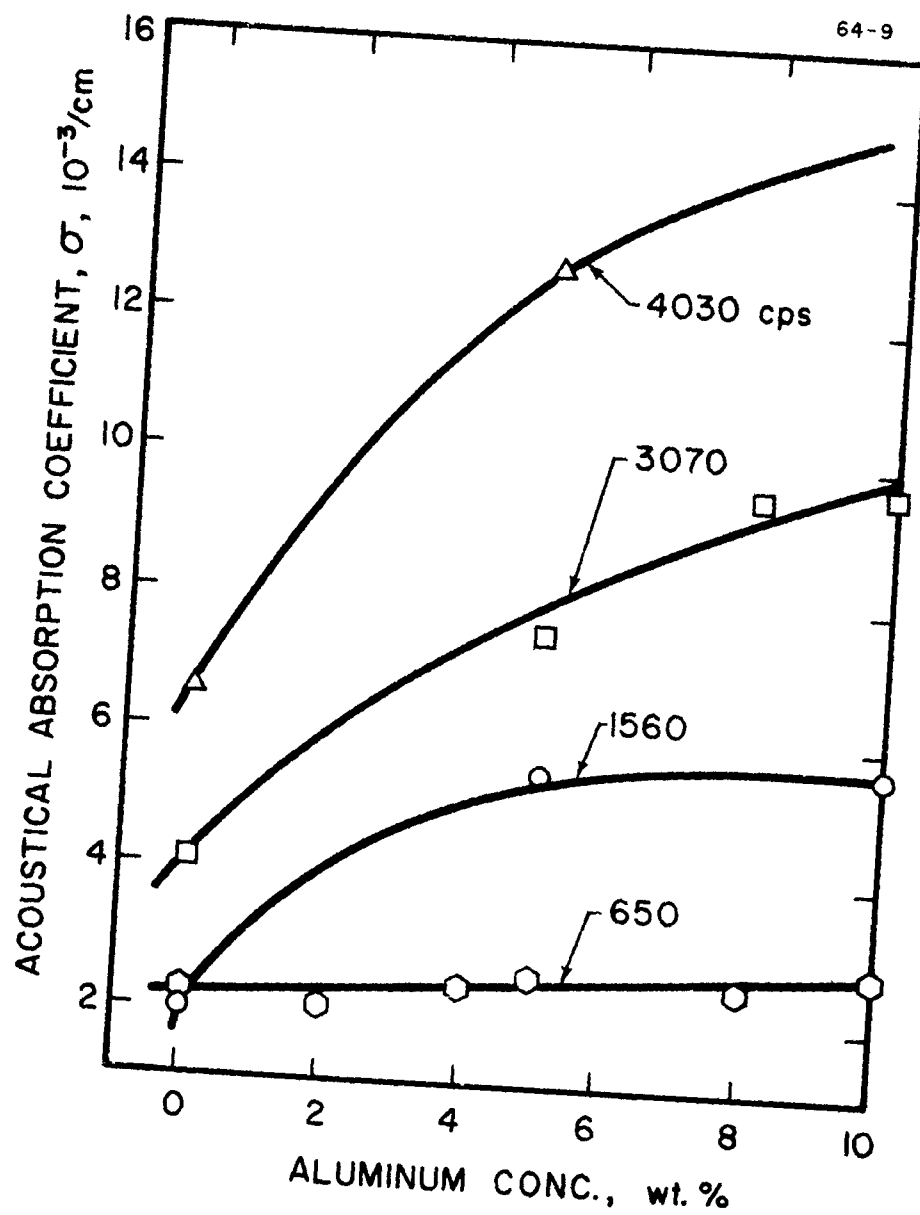


FIG. 6 EFFECT OF ALUMINUM CONCENTRATION ON ACOUSTICAL ABSORPTION COEFFICIENT

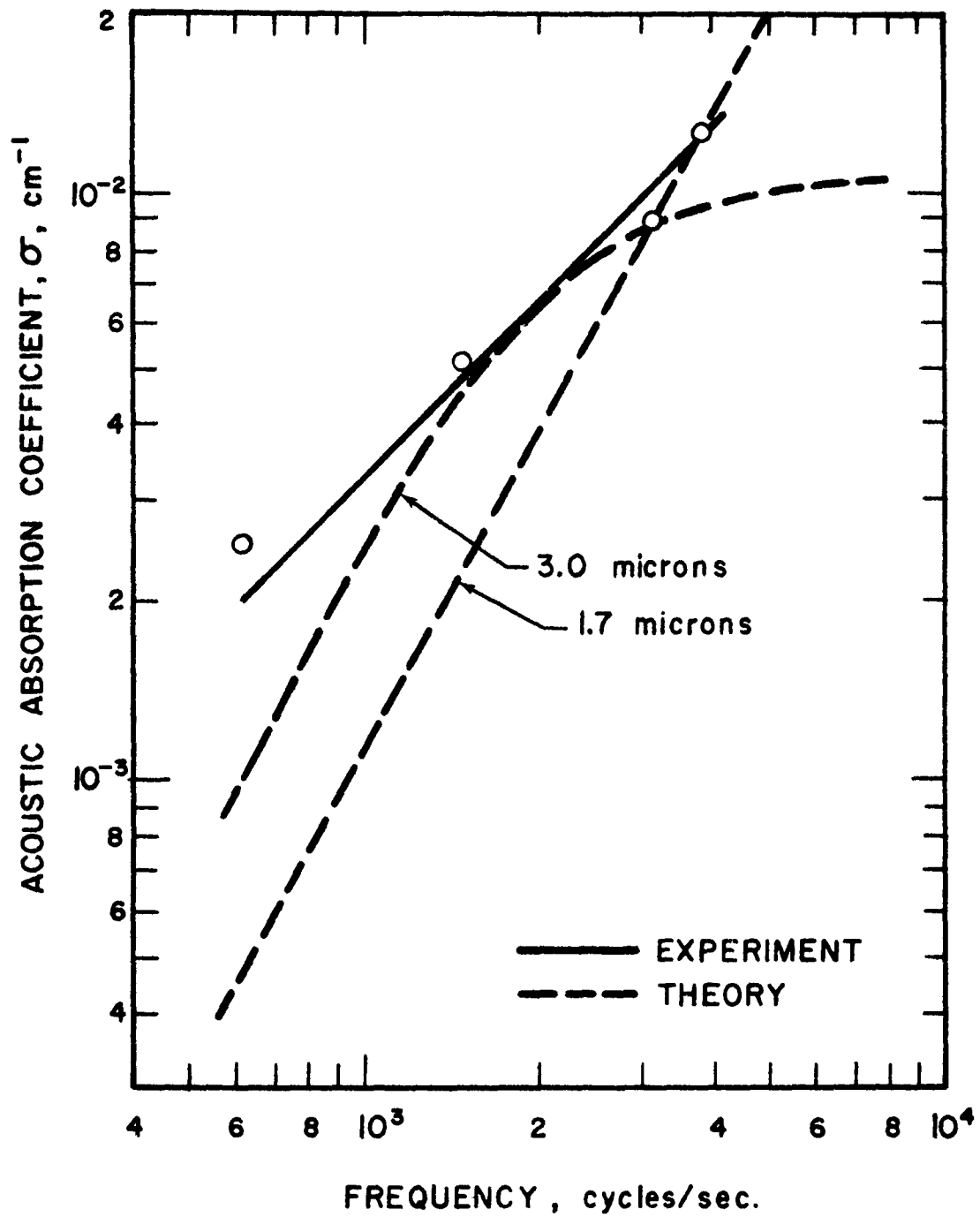


FIG. 7 COMPARISON OF EXPERIMENTAL AND THEORETICAL ACOUSTIC ABSORPTION COEFFICIENTS

Theoretical curves based on particle radii to fit experiment at 3070 cps  
5 wt. % Al,  $T = 2730^\circ\text{K}$

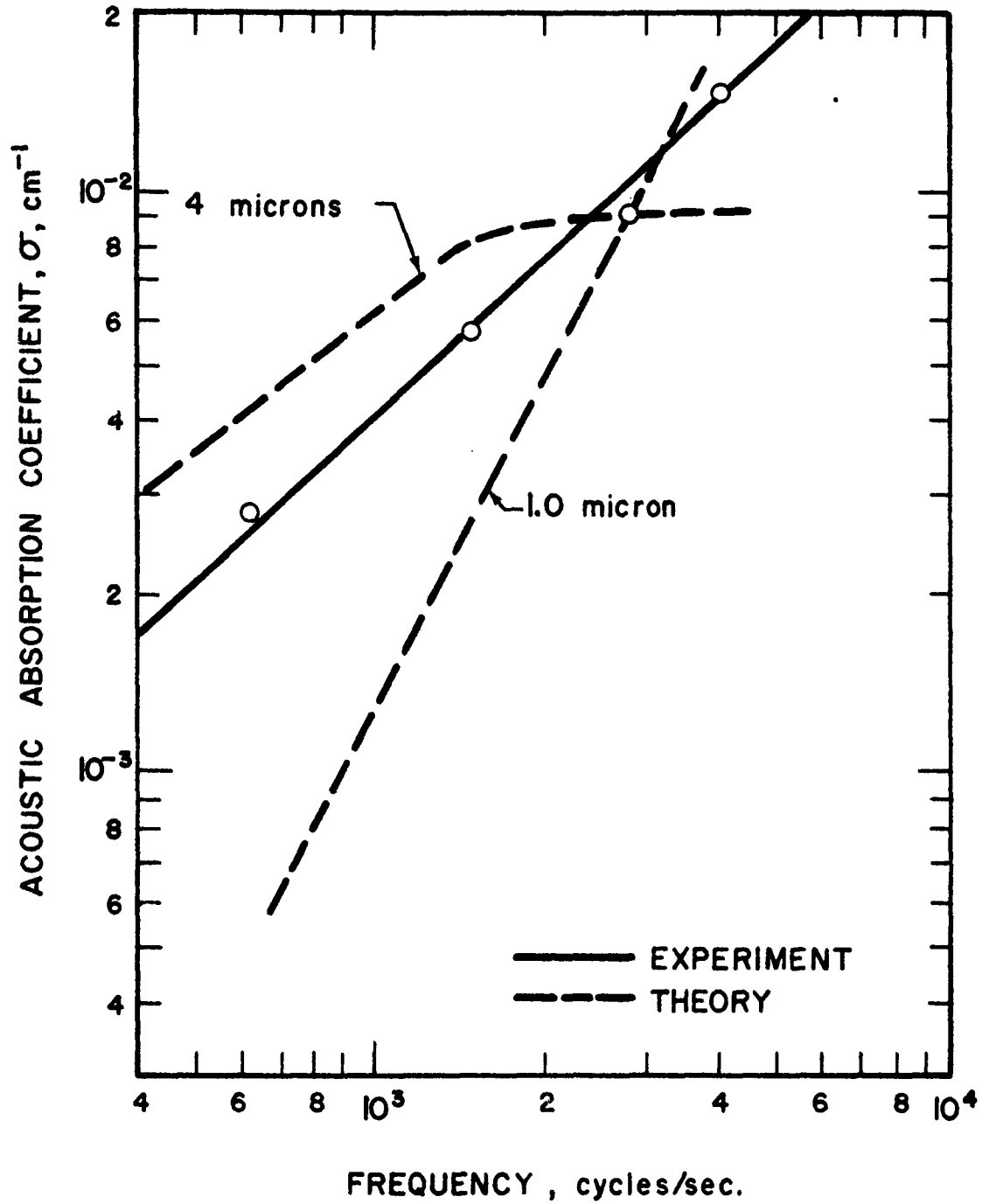


FIG. 8 COMPARISON OF EXPERIMENTAL AND THEORETICAL ACOUSTIC ABSORPTION COEFFICIENTS

Theoretical curves based on particle radii to fit experiment at 3070 cps  
5 wt. % Al,  $T = 2730^\circ\text{K}$

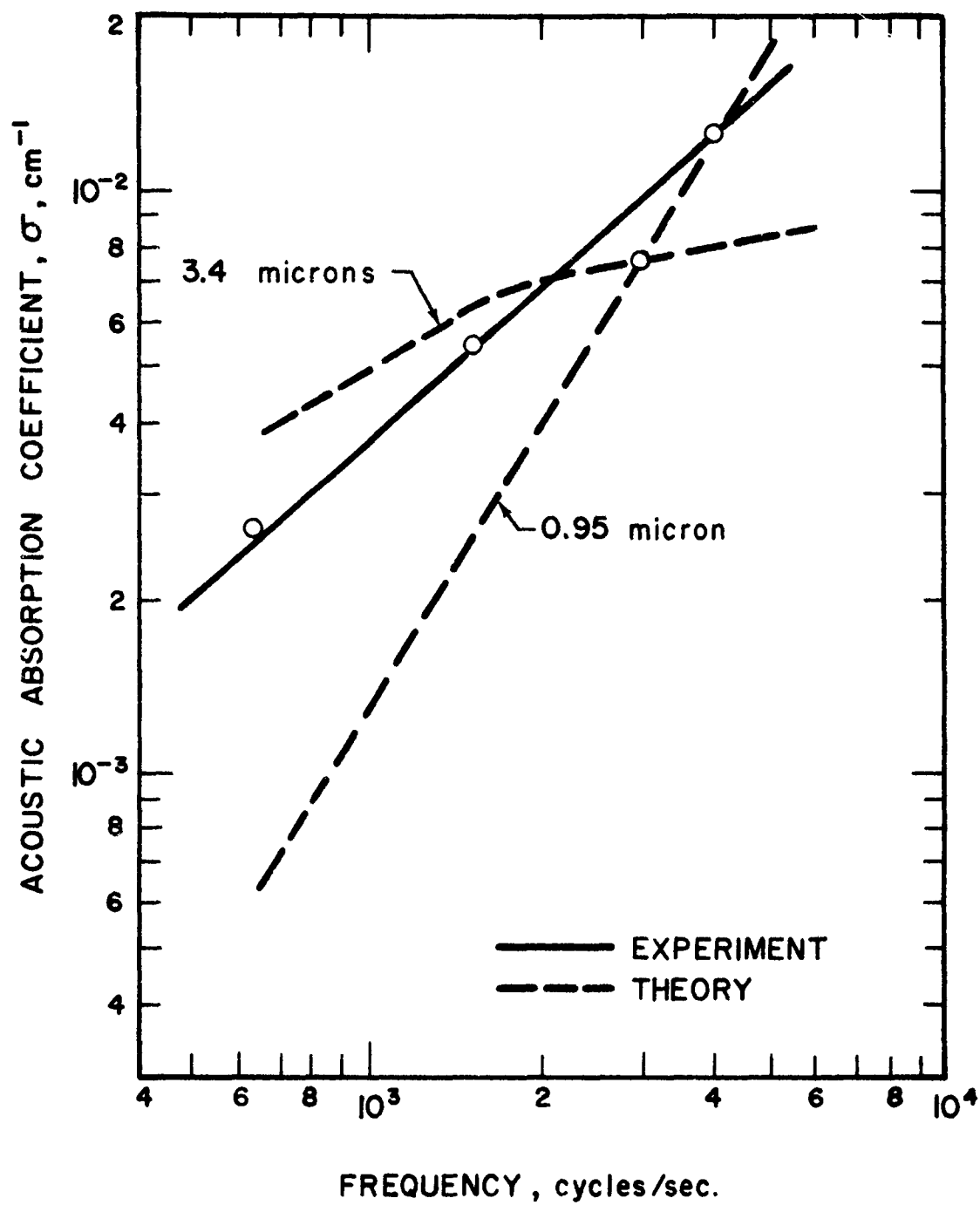


FIG. 9 COMPARISON OF EXPERIMENTAL AND THEORETICAL ACOUSTIC ABSORPTION COEFFICIENTS

Theoretical curves based on particle radii to fit experiment at 3070 cps  
5 wt. % Al,  $T = 1000^\circ\text{K}$

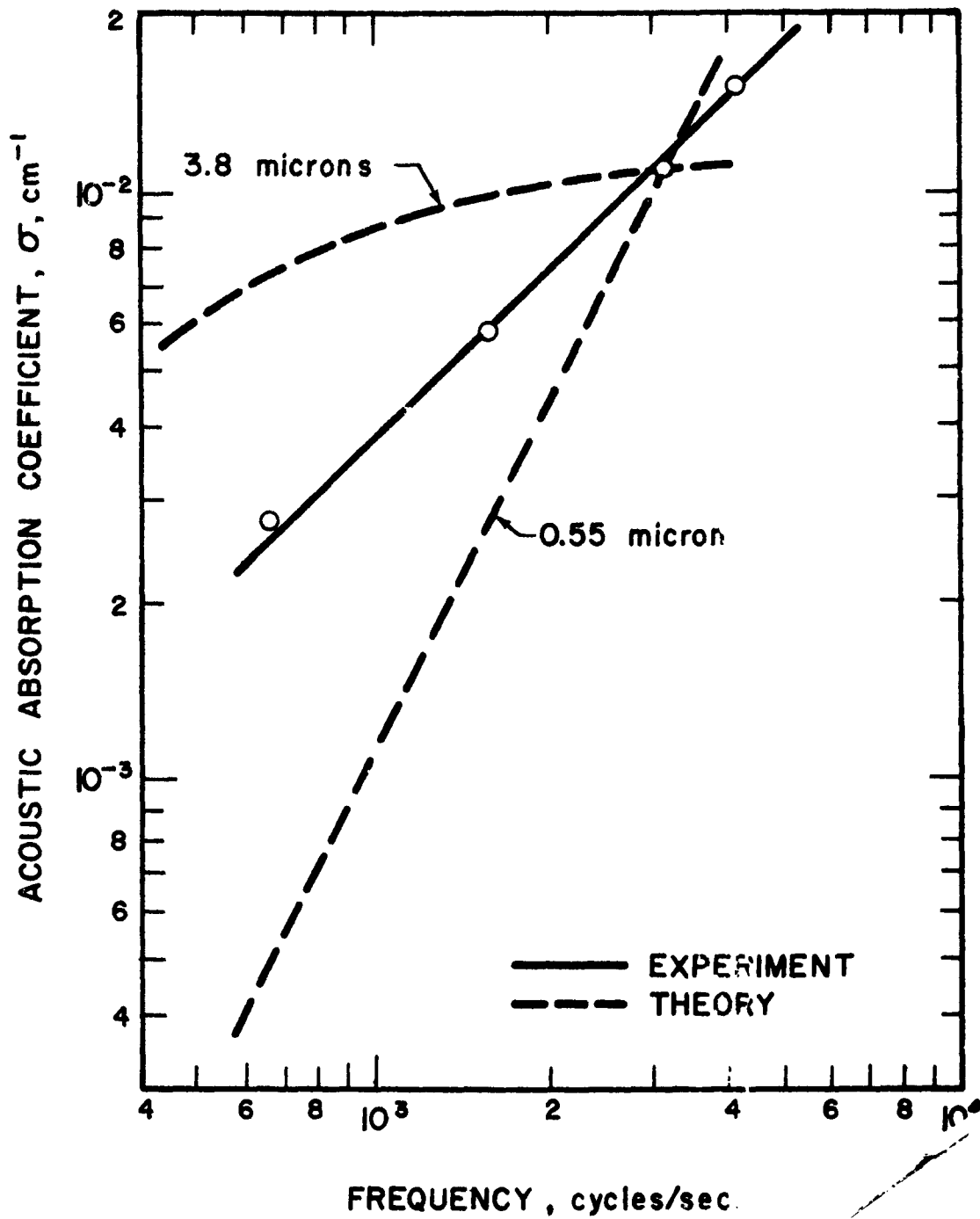


FIG. 10 COMPARISON OF EXPERIMENTAL AND THEORETICAL ACOUSTIC ABSORPTION COEFFICIENTS

Theoretical curves based on particle radii to fit experiment at 3070 cps  
10 wt. % Al,  $T = 1000^\circ\text{K}$

Unclassified  
Security Classification

DOCUMENT CONTROL DATA - R&D		
<i>(Security classification of title, body of abstract and indexing annotation must be entered when the overall report is classified)</i>		
1. ORIGINATING ACTIVITY (Corporate author) AeroChem Research Laboratories, Inc. P. O. Box 12 Princeton, New Jersey 08540	2. REPORT SECURITY CLASSIFICATION Unclassified	
3. REPORT TITLE ACOUSTIC ABSORPTION COEFFICIENTS OF THE COMBUSTION PRODUCTS OF ALUMINIZED PROPELLANTS		2. GROUP
4. DESCRIPTIVE NOTES (Type of report and inclusive dates)		
5. AUTHOR(S) (Last name, first name, initial) Ribnick, Authur and Calcote, Hartwell, F.		
6. REPORT DATE April 1965	7A. TOTAL NO. OF PAGES 33	7B. NO. OF REFS 5
8a. CONTRACT OR GRANT NO. Nonr 3477(00)	9. ORIGINATOR'S REPORT NUMBER(S) TP-112	
b. PROJECT NO. 9100	10. OTHER REPORT NUMBERS (Any other numbers that may be assigned this report)	
11. AVAILABILITY/LIMITATION NOTICES <p>Qualified requesters may obtain copies of this report from DDC.</p>		
12. SUPPLEMENTARY NOTES	13. SPONSORING MILITARY ACTIVITY Code 429 Office of Naval Research, Power Branch Dept. of the Navy Washington 25, D. C.	
14. ABSTRACT A resonance tube method has been used to measure the absorption of sound passed through a column of propellant gases and solid particles produced by the burning of small samples of aluminized propellant. Aluminum composition was varied to observe the effect of the increased quantity of alumina particles on sound absorption. The acoustical absorption coefficient increased with increasing aluminum concentration in the propellant. The absorption coefficient increased linearly with the frequency, consistent with the particulate damping theory of Epstein and Carhart. This theory was also used to estimate the sizes of alumina particles produced in the experiment. By a process of curve fitting, the inferred particle radii were either 0.80 or 3.5 microns, two solutions were possible. The initial average particle radius of the aluminum was 2.3. Despite the fact that a statistical distribution of particle size was not considered in curve-fitting the data, the reasonableness of the calculated particle sizes lend further support to the Epstein and Carhart theory.		

DD FORM 1473  
1 JAN 64

Unclassified  
Security Classification

14	KEY WORDS	LINK A		LINK B		LINK C	
		ROLE	WT	ROLE	WT	ROLE	WT

Acoustic Absorption  
Two-Phase Flow  
Rocket Motor Instability  
Aluminized Propellants

INSTRUCTIONS

1. **ORIGINATING ACTIVITY:** Enter the name and address of the contractor, subcontractor, grantee, Department of Defense activity or other organization (corporate author) issuing the report.

2a. **REPORT SECURITY CLASSIFICATION:** Enter the overall security classification of the report. Indicate whether "Restricted Data" is included. Marking is to be in accordance with appropriate security regulations.

2b. **GROUP:** Automatic downgrading is specified in DoD Directive 5200.10 and Armed Forces Industrial Manual. Enter the group number. Also, when applicable, show that optional markings have been used for Group 3 and Group 4 as authorized.

3. **REPORT TITLE:** Enter the complete report title in all capital letters. Titles in all cases should be unclassified. If a meaningful title cannot be selected without classification, show title classification in all capitals in parentheses immediately following the title.

4. **DESCRIPTIVE NOTES:** If appropriate, enter the type of report, e.g., interim, progress, summary, annual, or final. Give the inclusive dates when a specific reporting period is covered.

5. **AUTHOR(S):** Enter the name(s) of author(s) as shown in the report. Enter last name, first name, middle initial, and suffix. The name of the principal author is an absolute minimum. If military, show rank and service branch.

6. **REPORT DATE:** Enter the date of the report as day, month, year, or month-year. If more than one date appears on the report, use date of publication.

7a. **TOTAL NUMBER OF PAGES:** The total page count should follow normal pagination procedures, i.e., enter the number of pages containing information.

7b. **NUMBER OF REFERENCES:** Enter the total number of references cited in the report.

8a. **CONTRACT OR GRANT NUMBER:** If appropriate, enter the applicable number of the contract or grant under which the report was written.

8b, 8c, & 8d. **PROJECT NUMBER:** Enter the appropriate military department identification, such as project number, subproject number, system numbers, task number, etc.

9a. **ORIGINATOR'S REPORT NUMBER(S):** Enter the official report number by which the document will be identified and controlled by the originating activity. This number must be unique to this report.

9b. **OTHER REPORT NUMBER(S):** If the report has been assigned any other report numbers (either by the originator or by the sponsor), also enter this number(s).

10. **AVAILABILITY LIMITATION NOTICES:** Enter any limitations on further dissemination of the report, other than those

imposed by security classification, using standard statements such as:

- (1) "Qualified requesters may obtain copies of this report from DDC."
- (2) "Foreign announcement and dissemination of this report by DDC is not authorized."
- (3) "U. S. Government agencies may obtain copies of this report directly from DDC. Other qualified DDC users shall request through \_\_\_\_\_."
- (4) "U. S. military agencies may obtain copies of this report directly from DDC. Other qualified users shall request through \_\_\_\_\_."
- (5) "All dissemination of this report is controlled. Qualified DDC users shall request through \_\_\_\_\_."

If the report has been furnished to the Office of Technical Services, Department of Commerce, for sale to the public, indicate this fact and enter the price, if known.

11. **SUPPLEMENTARY NOTES:** Use for additional explanatory notes.

12. **SPONSORING MILITARY ACTIVITY:** Enter the name of the military project office or laboratory sponsoring (funding) the report. If more than one, list each in separate entries.

13. **ABSTRACT:** Enter a brief summary of the report. The abstract should be self-explanatory. It may also appear elsewhere in the body of the technical report. If additional space is required, a continuation sheet should be attached.

It is highly desirable that the abstract of classified reports be unclassified. Each paragraph of the abstract shall end with a indication of the military security classification of the information in the paragraph, represented as (TS), (S), (C), or (U).

There is no limitation on the length of the abstract. However, the suggested length is from 150 to 225 words.

14. **KEY WORDS:** Key words are technically meaningful terms or short phrases that characterize a report and may be used as index entries for cataloging the report. Key words must be selected so that no security classification is required. Identifiers, such as equipment model designation, trade name, military project code name, geographic location, may be used as key words but will be followed by an indication of technical content. The assignment of links, roles, and weights is optional.